Structure and Mechanical Properties of an O^{70} (*Fddd*) Network-Forming Pentablock Terpolymer

Adam J. Meuler,[†] Guillaume Fleury,[†] Marc A. Hillmyer,[‡] and Frank S. Bates*,[†]

Department of Chemical Engineering and Materials Science and Department of Chemistry, University of Minnesota, Minneapolis, Minnesota 55455

Received April 21, 2008; Revised Manuscript Received June 5, 2008

ABSTRACT: Symmetric poly(ethylene oxide-*b*-styrene-*b*-isoprene-*b*-styrene-*b*-ethylene oxide) (OSISO) pentablock terpolymers with narrow molecular weight distributions in all blocks were synthesized by anionic polymerization. These OSISO pentablock terpolymers have a common poly(styrene-*b*-isoprene-*b*-styrene) (SIS) core containing equal volume fractions of polyisoprene and polystyrene but having different lengths of terminal poly(ethylene oxide) (PEO) chains. Small-angle X-ray scattering, transmission electron microscopy, dynamic mechanical spectroscopy, and differential scanning calorimetry were used to identify two-domain lamellae, O^{70} (the orthorhombic *Fddd* network), and three-domain lamellae (LAM_3) in the OSISO materials; these morphologies were previously identified in poly(isoprene-*b*-styrene-*b*-ethylene oxide) (ISO) triblock terpolymers with comparable compositions. Mechanical tensile testing was employed to probe the consequences of adding different lengths of semicrystalline PEO to the ends of intrinsically tough SIS triblock. An OSISO sample with the LAM_3 mesostructure fractured in a brittle fashion at a strain of 0.06 while an OSISO containing the O^{70} network, in contrast, had a strain at failure of 1.3, even though the crystallinity of the terminal PEO blocks was above the brittle threshold established in other multiblock materials. This improved toughness is attributed to the combined effects of a triply continuous morphology and an intrinsically tough SIS core.

Introduction

Decades of theoretical and experimental investigations have led to an understanding of the physics governing the phase behavior of AB diblock copolymers.[1−5] Diblock copolymer phase behavior is controlled primarily by two parameters: volume fraction f_A and the product $\chi_{AB}N$, where χ_{AB} is the segment−segment interaction parameter and N the overall degree of polymerization (both χ_{AB} and N are measured with respect to a reference volume). Four equilibrium morphologies have been identified in AB diblocks: lamellae, hexagonally packed cylinders, spheres arranged on a BCC lattice, and the gyroid with $Ia\bar{3}d$ symmetry (herein called Q^{230}, where "Q" indicates a cubic unit cell and "230" refers to the number of the space group in the crystallographic tables[6]). (A fifth morphology, the orthorhombic *Fddd* network (herein called O^{70}, where "O" indicates an orthorhombic unit cell and "70" refers to the number of the space group in the crystallographic tables[6]), recently has been identified over a very narrow range of f_A and $\chi_{AB}N$.[7−9]) The regions where these morphologies are stable are often presented on a "universal" phase map defined by f_A and $\chi_{AB}N$.[1,3−5]

The basic physical principles elucidated from diblock copolymers are readily extended to other macromolecular architectures. Many studies comparing the phase behavior of AB diblocks and ABA triblocks have appeared in the literature, and lamellae, hexagonally packed cylinders, BCC spheres, and Q^{230} have been identified as equilibrium morphologies.[10−22] The phase boundaries, domain spacings, and order−disorder transition temperatures (T_{ODT}'s) shift only slightly in changing the architecture from AB diblocks to ABA triblocks, indicating such a change barely alters the free energy of the system. Matsen and Thompson provided a simple explanation for the similarity of the AB and ABA systems.[21] They noted, for the ABA triblock, that while the segments of the B chains near the interface stretch to minimize interfacial area, the middle of the B block adopts a relaxed conformation in the center of the domain. Consequently, the free energy of the melt does not significantly change when the ABA triblocks are snipped in the center of the relaxed B chains to produce a system of AB diblocks. They suggest that similar reasoning can be applied to higher-order multiblock copolymers (e.g., symmetric ABCBA pentablocks should behave like the homologous ABC triblocks).

The addition of a third chemically distinct block to form ABC triblock terpolymers significantly complicates matters, and more than 30 equilibrium mesostructures have been identified in such multiblocks.[23] This higher level of complexity derives from an increased number of molecular variables, including two independent composition variables, the overall degree of polymerization N, three χ_{ij}'s (χ_{AB}, χ_{AC}, and χ_{BC}), three statistical segment lengths (b_A, b_B, and b_C), and three distinct block sequences (ABC, ACB, BAC). While this large number of variables has prevented development of a "universal" ABC triblock phase map analogous to that created for AB diblocks, the complex phase behavior of ABC triblocks has motivated interest in harnessing these fascinating morphologies in practical applications.

We have extensively investigated the structure of poly(isoprene-*b*-styrene-*b*-ethylene oxide) (ISO) triblock terpolymers.[9,24−31] The interaction parameter between the I and O end blocks is the largest in this system ($\chi_{IO} > \chi_{IS} \approx \chi_{SO}$),[32] making formation of the optional (i.e., not required by chain connectivity) I/O interface enthalpically unfavorable; Bailey et al. described block terpolymers with this block sequence as "nonfrustrated".[33] The free energy associated with formation of the I/O interface drives ISO triblocks to adopt morphologies with two interfaces (the I/S and S/O interfaces required by chain connectivity) and promotes formation of network morphologies. Three network morphologies have been identified experimentally[24,26,27] and theoretically[9] in O-lean ($f_O < 0.30$) ISO triblocks: core−shell gyroid (Q^{230}), O^{70}, and an alternating gyroid with $I4_132$ symmetry (also called Q^{214}, where "Q" indicates a cubic unit cell and "214" refers to the number of the space group in the crystallographic tables[6]). Formation of

* To whom correspondence should be addressed. E-mail: bates@cems.umn.edu.
[†] Department of Chemical Engineering and Materials Science.
[‡] Department of Chemistry.

10.1021/ma800885s CCC: $40.75
Published on Web 07/19/2008

these ordered networks is sensitive to the polydispersity index (PDI = M_w/M_n, where M_w and M_n are the weight-average and number-average molecular weights) of the polystyrene (PS) block as well as the overall molecular weight of the triblocks. Lamellae, and not network mesostructures, were identified along the $f_I = f_S$ isopleth when the PS block PDI = 1.31.[31] The O^{70} network also was absent along the $f_I = f_S$ isopleth for high-molecular-weight ISO triblocks. Unlike with the increased PS block PDI, the elevated segregation strength did not result in the formation of a lamellar morphology. Instead, the high molecular weight ISO triblocks formed interpenetrating, triply periodic networks that lacked the translational order of O^{70}. Epps and Bates attributed this lack of order to kinetic limitations and suggested that O^{70} could still be the equilibrium mesostructure for these higher segregation strength ISO compounds,[29] a prediction supported by recent theoretical work.[34]

The percolating interconnected domains of the network morphologies identified in ISO triblocks and other ABC systems[33,35–40] could find utility in a number of applications requiring mechanical toughness, including use as a photonic crystal[41] or as a membrane (e.g., for gas separation[35] or, after degradation and removal of one of the blocks,[42] for water purification[43,44]). In some separation applications (e.g., water filtration), anisotropic morphologies like hexagonally packed cylinders may require costly and/or time-consuming alignment procedures to minimize pore dead ends and maximize flux through the membrane. The percolating domains of network morphologies, in contrast, are not likely to terminate at grain boundaries, rendering expensive alignment procedures unnecessary. Unfortunately, ISO triblocks are brittle materials, limiting their potential efficacy in many applications. Brittleness is common in ABC triblocks and is often the result of a rubbery end block(s); constraining a rubbery domain between glassy end blocks significantly improves mechanical toughness.[16]

In this article, the mechanical properties of ABC block terpolymers are enhanced by exploiting the ABCBA pentablock architecture, a strategy previously pursued by Kopchick et al. in poly(acrylic acid-*b*-styrene-*b*-isobutylene-*b*-styrene-*b*-acrylic acid) pentablock terpolymers.[45] This strategy requires an intrinsically tough BCB triblock, a constraint satisfied by symmetric poly(ethylene oxide-*b*-styrene-*b*-isoprene-*b*-styrene-*b*-ethylene oxide) (OSISO) pentablock terpolymers. Two-domain lamellae (LAM_2), O^{70}, and three-domain lamellae (LAM_3) are identified in the OSISO pentablocks. To the best of our knowledge, no network morphologies have previously been identified in ABCBA pentablocks. The terminal poly(ethylene oxide) (PEO) blocks do not enhance the mechanical properties of the SIS thermoplastic elastomer but potentially provide added functionality. For instance, PEO has been degraded to yield a nanoporous material[46,47] and used as a polymer electrolyte.[48–50] The mechanical consequences of adding the brittle PEO blocks to the termini of SIS are probed via tensile testing.

Experimental Section

Polymer Synthesis. The poly(ethylene oxide-*b*-styrene-*b*-isoprene-*b*-styrene-*b*-ethylene oxide) (OSISO) pentablock terpolymers were prepared by living anionic polymerization using a protected initiation strategy. All polymerizations were performed under an inert argon atmosphere following established techniques.[51] α,ω-Dihydroxypoly(styrene-*b*-isoprene-*b*-styrene) (HO-SIS-OH) triblocks were first prepared using the functional organolithium 3-triisopropylsilyloxy-1-propyllithium (TIPSOPrLi).[52] Ethylene oxide polymerizations were subsequently initiated from both ends of the HO-SIS-OH using potassium naphthalenide to yield the OSISO pentablocks. This reaction scheme is summarized in Figure 1, and the specific details of the procedure are described in the following paragraphs.

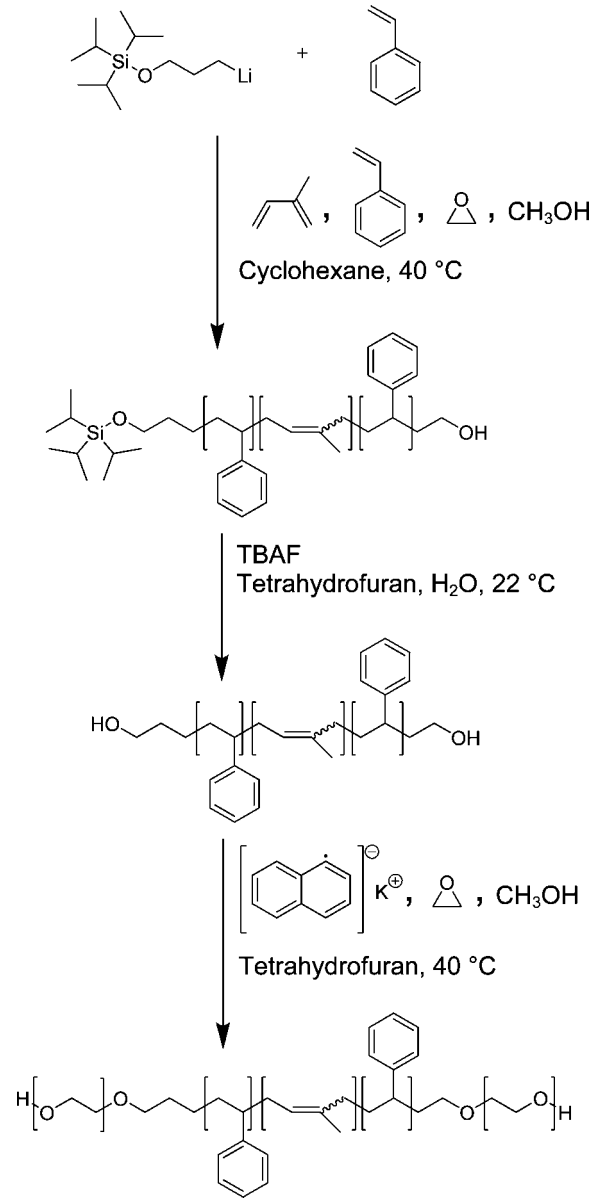

Figure 1. Synthetic scheme for the OSISO pentablock terpolymers.

Anionic polymerization of styrene in cyclohexane at 40 °C was initiated by TIPSOPrLi. TIPSOPrLi and cyclohexane (500 mL) were thermostated at 40 °C, and the initiator was "seeded" to minimize the breadth of the polystyrene (PS) molecular weight distribution.[52,53] To "seed" the initiator, three aliquots of styrene monomer (~0.5 g) were added in successive 20 min intervals before the balance of the styrene (12.7 g including initial aliquots) was added to the reactor. Living polystyryllithium chains (~3 mL of solution) were removed from the reactor, terminated via precipitation in degassed methanol, and analyzed using size exclusion chromatography (SEC) calibrated with PS standards to determine the M_n and M_w/M_n of the first PS block. Isoprene (21.9 g) and styrene (12.7 g) were subsequently sequentially added to the reactor and polymerized (all polymerizations lasted at least 8 h to ensure essentially complete conversion) before ethylene oxide (~2 g) was added to end-cap the triblocks with an oxanion. Degassed methanol (10 mL) was injected into the reactor to terminate the living chains and create terminal hydroxyl groups; the polymer was recovered via precipitation into methanol (~2 L).

The α-hydroxyl group was unmasked using tetra(*n*-butyl)ammonium fluoride (TBAF), and the HO-SIS-OH was recovered and

freeze-dried from benzene following an established protocol.[52] The α,ω-dihydroxy SIS triblock (~4 g) was dissolved in tetrahydrofuran (THF) (~300 mL) stirring at 40 °C, and ethylene oxide polymerizations were initiated from the terminal hydroxyl groups with potassium naphthalenide and terminated with degassed methanol (~5 mL) after reacting for at least 40 h. The OSISO pentablocks were subsequently dissolved in dichloromethane and washed with distilled water to remove excess salts in accordance with reported procedures.[33,54] The OSISO pentablocks were recovered from the dichloromethane solution by precipitation in isopropanol and were then freeze-dried from benzene. SEC traces of the OSISO pentablocks revealed no evidence of PS homopolymers, IS diblocks, or parent SIS triblocks.

Molecular Characterization. The compositions of the OSISO pentablocks were determined using a 300 MHz Varian NMR instrument operating at room temperature with deuterated chloroform as the solvent. Block mole fractions were calculated using the integrated ^{1}H NMR spectra and converted to volume fractions f_I, f_S, and f_O using published homopolymer densities at 140 °C ($\rho_I = 0.830$, $\rho_S = 0.969$, $\rho_O = 1.064$ g/cm^3).[55]

Room temperature SEC analyses employing THF as the mobile phase (flow rate 1.0 mL/min) were performed on a Waters 717 GPC equipped with three Polymer Laboratories Mixed-C columns and a Waters 410 differential refractometer. A calibration curve constructed using 10 PS standard samples with M_n ranging from 580 to 377 400 g/mol (Polymer Laboratories) was used to determine M_w/M_n of all polymers. SEC analysis of the PS in the aliquot removed from the reactor provided M_n of the initiated PS block; M_n values of the SIS triblocks were computed using the M_n of the initiated PS block and the masses of isoprene and styrene subsequently added to the reactor. Actual compositions were verified by ^{1}H NMR spectroscopy and in all cases indicated that complete addition of isoprene and styrene monomers had been achieved. OSISO M_n values were calculated from M_n of the SIS triblocks and the overall compositions measured using ^{1}H NMR spectroscopy.

Synchrotron Small-Angle X-ray Scattering (SAXS). Synchrotron SAXS experiments were conducted at Argonne National Laboratory using the equipment maintained by the DuPont-Northwestern-Dow Collaborative Access Team (DND-CAT). Two equipment setups (yielding equivalent data for our purposes) were employed: (1) an X-ray wavelength (λ) of 1.032 Å with a sample-to-detector distance of 2.01 m and (2) $\lambda = 0.886$ Å with a sample-to-detector distance of 5.47 m. Both distances were calibrated with silver behenate, and data were acquired on a Mar CCD area detector. Sample temperatures were controlled using a liquid-nitrogen-cooled differential scanning calorimetry (DSC) chamber under a helium purge. All samples were heated 10 °C above T_{ODT} (when possible) or to 250 °C for 5 min before data were acquired in an effort to erase effects due to thermal history. Samples were cooled and held at target temperatures for 5 min before data were collected. 2-D diffraction intensities were azimuthally averaged, and data are presented in this article as plots of intensity (I) as a function of the scattering wave-vector modulus ($q = |\mathbf{q}| = 4\pi/\lambda \sin(\theta/2)$, where θ is the scattering angle).

Transmission Electron Microscopy (TEM). TEM micrographs were obtained using a JEOL 1210 TEM operating at 120 kV located in the University of Minnesota Institute of Technology Characterization Facility. Samples were compression-molded between Teflon sheets into bars 0.5−1 mm thick using a pressure of 500−1000 psi at 100 °C for 5 min. The molds were placed in a vacuum oven and annealed ~10 °C below T_{ODT} for ~ 4 h, cooled to 80 °C for ~1 h, and then cooled to room temperature. Sample slices (50−100 nm thickness) were prepared using a Reichart ultramicrotome fitted with a Microstar diamond knife operated at −120 °C. Slices were placed on copper grids (Ted Pella) and stained through exposure to the vapor from a 4% aqueous solution of OsO_4 for 3−5 min (10 min for SIS). The metal oxide selectively reacts with the olefinic groups present in the polyisoprene (PI) and enhances electron mass density contrast.

Dynamic Mechanical Spectroscopy (DMS). DMS experiments were conducted on a Rheometrics Scientific ARES strain-controlled rheometer equipped with 25 mm diameter parallel plates. Polymers were compression-molded between Teflon sheets into 1 mm thick disks using a pressure of 500−1000 psi at 100 °C for 5 min. The disks were placed in the rheometer and heated in a nitrogen atmosphere 10 °C above T_{ODT} or to 250 °C for 10 min in an effort to erase effects due to thermal history. Isochronal ($\omega = 1$ rad/s) dynamic elastic (G') and loss (G'') moduli measurements were obtained while heating or cooling at 1 °C/min. Isothermal frequency (ω) sweeps between $\omega = 10^2$ and 10^{-1} rad/s were conducted to probe the viscoelastic behavior at specific temperatures. All data were acquired using a low strain amplitude (1−2%) that was determined to be within the linear viscoelastic regime.

Tensile Testing. Samples were compression-molded between Teflon sheets into 0.5 mm thick bars at 500−1000 psi and 100 °C for 5 min. These master bars had a rectangular cross section measuring 17 × 13 mm and were stored at −26 °C. Prior to tensile testing, the master bars were removed from the freezer, allowed to warm to room temperature, and cut into rectangular tensile bars measuring 13 mm × 2.5 mm × 0.5 mm using a fresh razor blade. Uniaxial tensile tests were carried out at room temperature using a Rheometrics Scientific MINIMAT equipped with a 200 N load cell. The MINIMAT operated with a crosshead speed of 8 mm/min and an initial gauge length of 8 mm (length-independent strain rate of 1 min^{-1}) for all samples except ISO-7a; the tensile tests for this brittle material were performed using a crosshead speed of 1 mm/min and an initial gauge length of 8 mm. The force−displacement measurements were converted to engineering stress $\sigma = F/A_0$ vs nominal strain $\varepsilon = (l - l_0)/l_0$, where l is the length of the sample and A_0 and l_0 are the initial cross-sectional area and length of the sample, respectively. All reported values are averages from at least four independent trials.

Differential Scanning Calorimetry (DSC). Calorimetry experiments were conducted with a TA Instruments Q1000 DSC. Portions of the master tensile bar that had been stored in the freezer were used for the DSC experiments. 8 ± 1 mg of polymer was placed into aluminum DSC pans, and data were acquired while heating the samples from 20 to 150 °C at 10 °C/min. Three separate DSC pans were examined for each sample.

Results and Analysis

Four symmetric polymers with narrow overall molecular weight distributions were synthesized along the $f_I = f_S$ isopleth: a parent SIS triblock and three OSISO pentablocks. The molecular characterization data obtained from these samples are provided in Table 1. An aliquot of the first PS block was extracted from the reactor during SIS synthesis and analyzed using SEC; this first PS block had $M_n = 6.8$ kg/mol with $M_w/M_n = 1.13$. The overall molecular weights were computed using this M_n value and the ^{1}H NMR spectra of the final polymers. The morphology assignments, lattice dimensions, and T_{ODT}'s were obtained using a combination of DMS, TEM, and SAXS.

The characterization data from two previously studied[24,26,27,29] series of ISO triblocks are also reproduced in Table 1. The lower segregation strength ISO triblocks have approximately half the overall molecular weight of the OSISO pentablocks, and the phase behavior of these two series is expected to be similar.[21] The higher segregation strength ISO polymers have overall molecular weights comparable to the OSISO pentablocks, allowing us to isolate the influence of chain architecture on the mechanical tensile properties.

SAXS. Synchrotron SAXS powder patterns for the OSISO pentablocks and the ISO-7a triblock are presented in Figure 2. Data for SIS were collected at 85 °C, data for OSISO(0.06) were obtained at 100 °C, and data for OSISO(0.13), OSISO(0.35), and ISO-7a were acquired at 160 °C; these temperatures were targeted to facilitate comparison of lattice dimensions between the OSISO pentablocks and the previously reported[24,27] ISO

Table 1. OSISO and ISO Characterization Data

polymer	f_I[d]	f_S[d]	f_O[d]	M_n (kDa)	N[e]	M_w/M_n	lattice dimensions (nm)[f]	morphology	T_{ODT}[g] (°C)
SIS[a]	0.50	0.50	0	25.5	399	1.08	15.3 (85 °C)	LAM_2	122
OSISO(0.06)[a]	0.47	0.47	0.06	27.3	424	1.10	16.7 (110 °C)	LAM_2	172
OSISO(0.13)[a]	0.44	0.43	0.13	29.9	458	1.10	0.293, 0.577, 73.2	O^{70}	237
OSISO(0.35)[a]	0.33	0.32	0.35	41.5	612	1.07	25.0	LAM_3	>250
IS-OH3[b]	0.50	0.50	0	13.6	212	1.05	15.8 (85 °C)	LAM_2	97
ISO2[b]	0.47	0.47	0.06	14.6	226	1.06	16.9 (110 °C)	LAM_2	146
ISO4[b]	0.44	0.44	0.12	15.8	242	1.05	0.294, 0.582, 65.4	O^{70}	194
ISO12[b]	0.33	0.33	0.34	21.8	321	1.06	25.3	LAM_3	>300
ISO-7a[c]	0.43	0.42	0.15	30.2	460	1.05	0.301, 0.580, 97.4	O^{70}	>250
ISO-7b[c]	0.41	0.39	0.20	32.4	489	1.06	26.8	network	>250

[a] M_w/M_n value for the first PS block is 1.13. [b] Polymers were previously synthesized and characterized[24,27] and are labeled using the nomenclature of Bailey et al.[24] The M_w/M_n value for the PS block in this series is 1.08.[31] [c] Polymers were previously synthesized and characterized by Epps and Bates and are labeled using their nomenclature.[29] [d] Volume fractions are calculated from published density values at 140 °C ($\rho_I = 0.830$, $\rho_S = 0.969$, $\rho_O = 1.064$ g/cm^3).[55] [e] Based on a segment reference volume of 118 Å^3. [f] Lattice dimensions are obtained from SAXS data and are reported at 160 °C unless otherwise noted in parentheses (°C). The lattice dimensions listed for O^{70} correspond to *a*/*c*, *b*/*c*, and *c*, and the value listed for ISO-7b corresponds to the length scale associated with the primary scattering vector. [g] Measured using DMS.

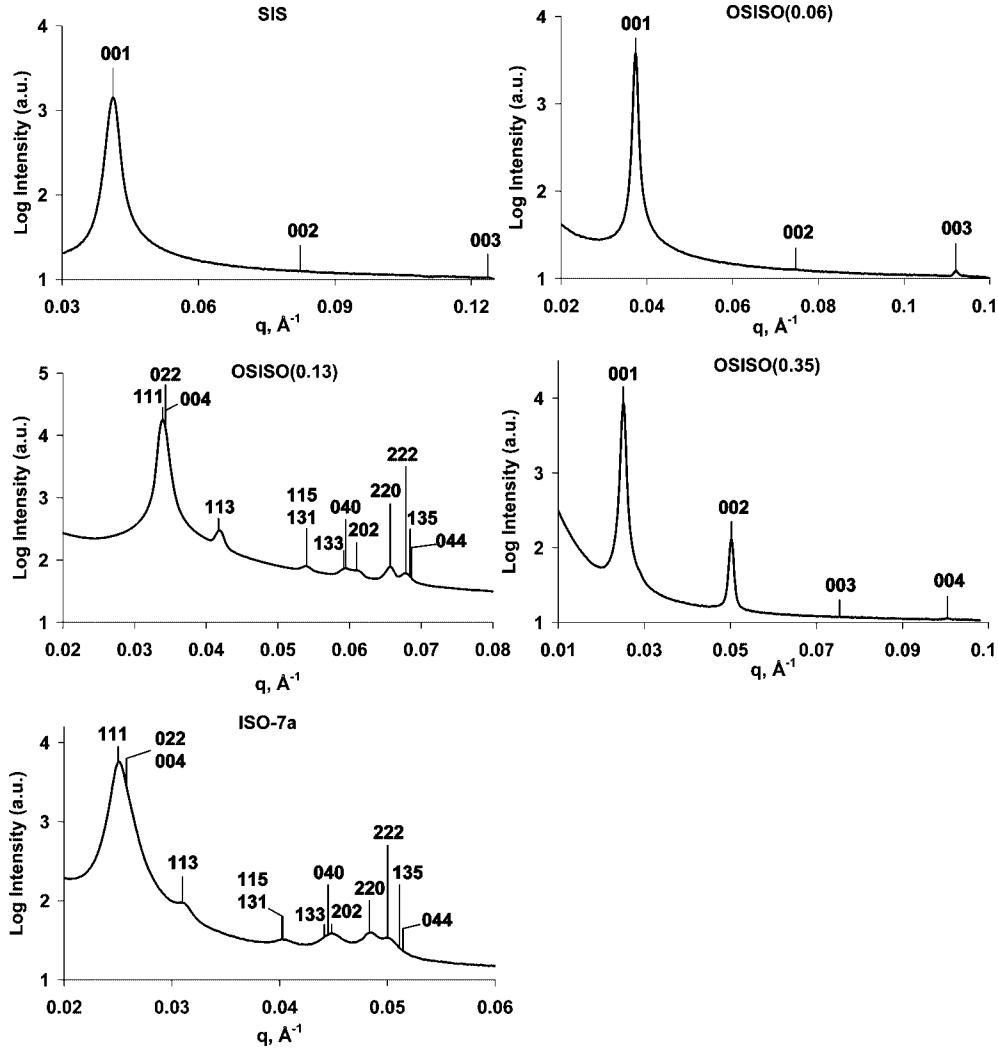

Figure 2. Synchrotron SAXS data acquired at 85 °C (SIS), 100 °C (OSISO(0.06)), or 160 °C (OSISO(0.13), OSISO(0.35), and ISO-7a). All samples were annealed 10 °C above T_{ODT} for 5 min (at 250 °C for OSISO(0.35) and ISO-7a) before data were collected. The data for SIS, OSISO(0.06), and OSISO(0.35) are indexed to a lamellar morphology, while the diffraction patterns for OSISO(0.13) and ISO-7a are indexed to O^{70}. The absences of the 002 peak in SIS and OSISO(0.06) and the 003 peak in OSISO(0.35) are consistent with structure factor extinctions for symmetric LAM_2 and symmetric LAM_3, respectively.[27]

triblocks. The SAXS peaks for SIS, OSISO(0.06), and OSISO(0.35) are indexed to a lamellar morphology. The absences of the 002 peak for SIS and OSISO(0.06) and of the 003 peak for OSISO(0.35) are consistent with structure factor extinctions for symmetric LAM_2 and symmetric LAM_3, respectively.[27] The rich assortment of diffraction peaks for OSISO(0.13) and ISO-7a are indexed to O^{70}. The allowed reflections for the orthorhombic lattice are not simple multiples of the primary peak q^*, as they are for cubic lattices, but vary with the lattice dimensions *a*, *b*, and *c* according to $q_{hkl} = 2\pi[h^2/a^2 + k^2/b^2 + l^2/c^2]^{1/2}$, where *h*, *k*, and *l* are the associated Miller indices. The values of *a*, *b*, and *c* were varied to obtain the best least-squares lattice parameters reported in Table 1; the reported *a*/*c*, *b*/*c*, and *c* values lead to the indexing scheme presented in Figure 2.

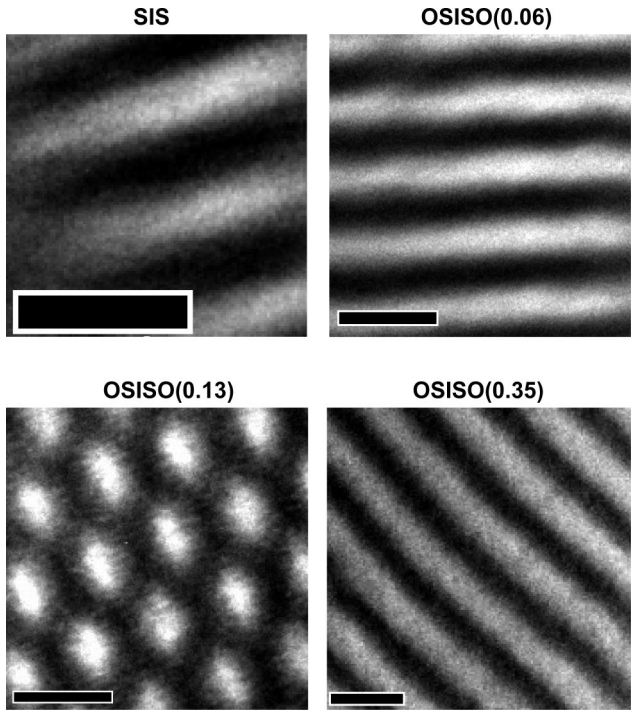

Figure 3. TEM micrographs of SIS and the OSISO pentablocks. Dark regions in the TEM micrographs result from OsO_4 staining of the PI domains. The unstained PS and PEO appear much lighter. Scale bars correspond to 20 nm.

TEM. Selected TEM micrographs of the SIS triblock and the OSISO pentablocks are presented in Figure 3. Dark sections correspond to OsO_4-stained PI domains while the white areas are unstained PS and/or PEO regions. The alternating white and dark stripes in the SIS, OSISO(0.06), and OSISO(0.35) images are domains of the lamellar mesostructures; the white stripes are thicker than the black ones for OSISO(0.35) as they account for both the PS and PEO domains in this LAM_3 morphology. The TEM micrograph of OSISO(0.13) does not contain the alternating stripes of lamellae but consists of rows of slightly ellipsoidal white separated by gray connections. This micrograph is consistent with the [101] projection of the O^{70} space group.[27] All of the TEM images are consistent with the morphology assignments made using the SAXS data.

DMS. Isochronal dynamic elastic moduli (G') measurements obtained while heating a specimen (not shown) were used to identify the order−disorder transition temperatures (T_{ODT}) of SIS and the OSISO pentablocks; T_{ODT} is associated with the temperature at which G' discontinuously decreases upon heating a polymer.[56] No discontinuous increases or decreases in G' or G'' were observed while heating the polymers from 100 °C to just below T_{ODT}, which we interpret as an absence of order−order transitions prior to disordering. T_{ODT} values are listed in Table 1 for samples SIS, OSISO(0.06), and OSISO(0.13). Samples OSISO(0.35), ISO-7a, and ISO-7b remained ordered up to 250 °C, the highest temperature accessed during these measurements. Both the T_{ODT} values and the lack of order−order transitions are consistent with the SAXS results.

The linear viscoelastic behavior of the polymers was investigated using isothermal frequency sweeps. The time−temperature superimposed (TTS) responses of SIS and the OSISO pentablocks are provided in Figure 4. Kossuth and co-workers have demonstrated that the low-frequency G' response is sensitive to the nature of the periodic order.[57] A plateau in G' ($G' \sim \omega^0$) indicates solidlike behavior that is characteristic of triply periodic morphologies such as Q^{230}, O^{70}, or BCC spheres. The plateau in G' for OSISO(0.13) is consistent with the triply periodic O^{70} network.[27] G' of singly and doubly periodic morphologies such as lamellae or cylinders decreases with decreasing ω; the SIS, OSISO(0.06), and OSISO(0.35) responses are all consistent with a lamellar morphology.

DSC. The fractional crystallinity of the PEO block (X_c) was calculated for each sample from the heat of melting (ΔH_m) measured by DSC, based on

$$X_c = \Delta H_m / w_{PEO} \Delta H^\circ_{m,PEO}$$

where w_{PEO} is the weight fraction of PEO in the block terpolymer and $\Delta H^\circ_{m,\ PEO}$ is the heat of fusion of bulk PEO (213 J/g).[58] The X_c's were calculated from data obtained during the first heating of a specimen with the same thermal history (compression-molded, stored at −26 °C, and warmed to room temperature) as the samples that underwent tensile testing; the values are listed in Table 2.

Tensile Testing. The tensile properties of block copolymers depend on composition, block architecture, and morphology. Representative engineering stress (σ) vs nominal strain (ε) curves are presented in groups in Figure 5 to facilitate discussion of the effects induced by varying these parameters. A summary of the tensile properties is provided in Table 2. Here we note that in all cases failure of the specimens occurred in close proximity to the grips, suggesting the reported values for the stress at break (σ_{fail}) and the strain at break (ε_{fail}) represent lower bounds for these materials. Values of Young's modulus (E) are not included in Table 2. While Young's modulus values are readily obtained from the slope of the σ vs ε plot at low strains, the instrument and test specimens were not configured to produce optimal linear results at low strains. As a result, the values obtained from multiple MINIMAT experiments were not statistically meaningful (±50%), although the magnitudes were consistent with previously reported Young's moduli for SIS triblocks ($E \approx 25-150$ MPa).[59–61] Since this study focuses on fracture, additional measurements of Young's moduli were not pursued.

Discussion

Synthetic Strategy. A synthetic route for preparing symmetric OSISO pentablock terpolymers with narrow molecular weight distributions in all blocks was described in the Experimental Section. The combination of the TIPSOPrLi protected initiator and ethylene oxide end-capping can be used to synthesize a variety of α,ω-dihydroxy block copolymers (or homopolymers) by anionic polymerization. Subsequent polymerizations can be initiated from these hydroxyl groups, and these reactions could proceed via a anionic, atom transfer radical (ATRP),[62] or ring-opening[63] mechanisms.

Morphology. Epps and Bates previously described the morphology of both ISO-7a($f_O = 0.15$) and ISO-7b($f_O = 0.20$) as a triply periodic "network" that lacked long-range translational order.[29] While the morphology assignment for ISO-7b is the same in this report, the O^{70} mesostructure is now assigned to ISO-7a. This assignment was made using the synchrotron SAXS data presented in Figure 2; the reflections in this figure are indexed to O^{70}. Epps and Bates annealed both ISO-7a and ISO-7b at 200 °C and only observed two broad reflections in the SAXS data. These broad peaks were consistent with a lack of translational order, and Epps and Bates attributed this feature to kinetic limitations associated with the relatively high segregation strengths of the polymers. They hypothesized that, absent kinetic limitations, well-formed grains of O^{70} could form. We annealed the samples at 250 °C for 5 min and obtained the well-defined Bragg peaks characteristic of O^{70} for sample ISO-7a. Heating ISO-7a to 250 °C decreased the segregation strength and increased the chain mobility, enabling the sample to adopt

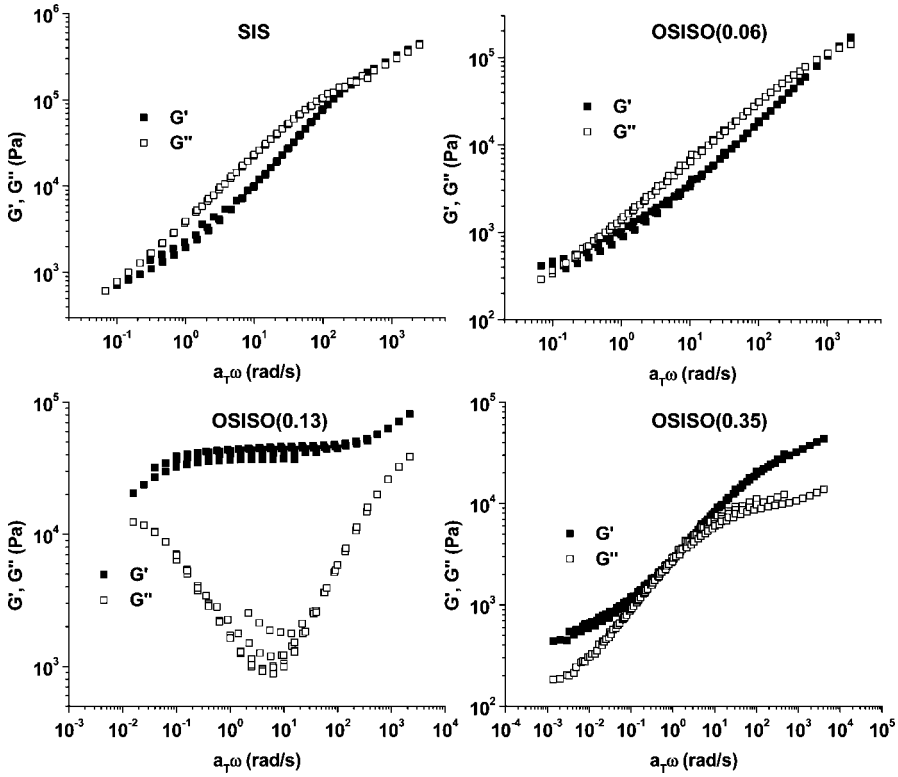

Figure 4. Superposition of isothermal frequency responses at 100, 110, and 120 °C (SIS, T_{ref} = 120 °C), 100, 115, 130, 145, and 160 °C (OSISO(0.06), T_{ref} = 130 °C), 120, 145, 170, 195, and 220 °C (OSISO(0.13), T_{ref} = 170 °C), and 100, 125, 150, 175, 200, 225, and 250 °C (OSISO(0.35), T_{ref} = 150 °C).

Table 2. PEO Crystallinities and Tensile Properties of SIS, the OSISO Pentablocks, and Triblock ISO-7a

sample	morphology	X_c, PEO	σ_{yield} (MPa)	ε_{fail}	σ_{fail} (MPa)
ISO-7a(f_O = 0.15)	O^{70}	0.57		0.02 ± 0.01	0.8 ± 0.1
OSISO(0.35)	LAM_3	0.76		0.06 ± 0.01	4.2 ± 0.6
OSISO(0.13)	O^{70}	0.29	4.2 ± 0.5	1.3 ± 0.2	4.2 ± 0.3
OSISO(0.06)	LAM_2	0.06	3.1 ± 0.2	2.2 ± 0.5	2.7 ± 0.3
SIS	LAM_2		3.8 ± 0.4	3.7 ± 0.6	6.2 ± 0.7

the (presumably equilibrium) O^{70} microstructure. The 250 °C heat treatment did not alter the state of order of sample ISO-7b, leading us to keep Epps and Bates' original "network" assignment.

Relatively few investigations of symmetric ABCBA pentablock terpolymers have appeared in the literature.[45,62,64–76] Previous reports have focused on synthetic methodology,[64–67,69] hydrogel[72,76] or ion gel[75] formation, and micellization in solvents.[62,68,70,71] Only a few reports have interrogated ABCBA pentablock terpolymers in the bulk.

Kopchick and co-workers have, to the best of the authors' knowledge, published the only previous investigation of bulk ABCBA pentablock terpolymers containing nonlamellar morphologies. These researchers examined poly(acrylic acid-*b*-styrene-*b*-isobutylene-*b*-styrene-*b*-acrylic acid) pentablock terpolymers that self-assembled into ordered, nonlamellar mesostructures. Definitive morphology assignments proved elusive, however.[45] Poly(acrylic acid-*b*-styrene-*b*-isobutylene) triblocks were not extensively characterized, preventing Kopchick et al. from comparing the phase behavior of ABC triblock and ABCBA pentablock terpolymers. The OSISO system, in contrast, is an extension of well-characterized ISO triblocks, facilitating comparison of the phase behavior of the respective architectures.

Mahanthappa and co-workers prepared poly(cyclohexylethylene-*b*-(ethylene-*alt*-propylene)-*b*-ethylene-*b*-(ethylene-*alt*-propylene)-*b*-cyclohexylethylene) (CPEPC) pentablock and CPE triblock terpolymers.[73,74] All of these block terpolymers contained lamellar mesostructures, including a CPEPC pentablock and its homologous CPE triblock. Pentablock CPEPC-50 (M_n = 30.9 kg/mol and T_{ODT} = 208 °C) and its homologous CPE-50 triblock (M_n = 16.2 kg/mol and T_{ODT} = 168 °C) both adopted lamellar morphologies, with CPEPC-50 having a higher T_{ODT} (208 °C) and larger domain spacing (20.0 nm) than CPE-50 (168 °C, 17.9 nm).[73]

The ISO system exhibits rich phase behavior[24,26,27] and the ability of OSISO pentablocks to adopt the same complex network morphologies was unknown. The identification of the O^{70} network for sample OSISO(0.13) proves that pentablock terpolymers can form network microstructures. SIS, OSISO(0.06), and OSISO(0.35) also adopt the same lamellar mesostructures as the homologous ISO counterparts (i.e., the lower molecular weight ISO triblocks summarized in Table 1). These results, along with those of Mahanthappa et al.,[73] support Matsen and Thompson's hypothesis that symmetric ABCBA pentablocks adopt the same morphologies as the homologous ABC counterparts.[21]

In addition to the identity of the ordered equilibrium mesostructure, the T_{ODT} and domain spacing are important parameters describing phase behavior. In the analogous AB and ABA systems, the ABA triblocks have higher T_{ODT}'s than their homologous AB diblocks,[13,22] a result in agreement with self-consistent-field theory calculations.[21] AB diblocks disorder at lower temperatures because the dangling B chain ends of the AB diblock can more readily penetrate A domains than the middle B segment of the ABA triblock.[21] OSISO(0.06) and

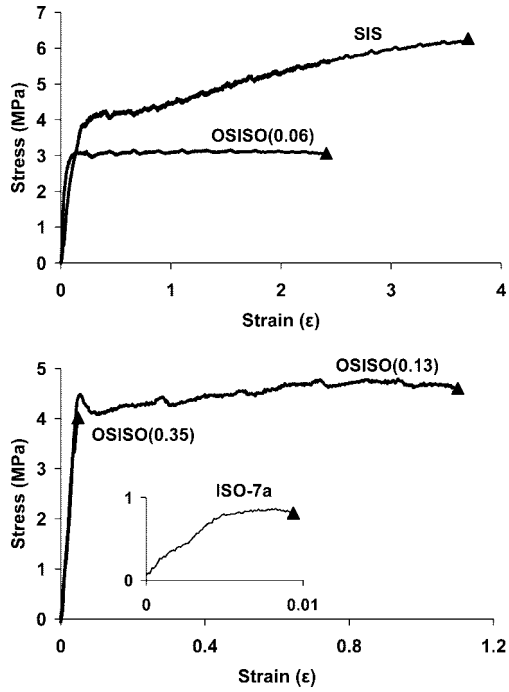

Figure 5. Representative engineering stress (σ) vs nominal strain (ε) curves for SIS, the OSISO pentablocks, and ISO-7a. Sample failures are marked by ▲.

OSISO(0.13) both have higher T_{ODT}'s than the homologous ISO triblocks (see Table 1); these results are consistent with the CPE/CPEPC data reported by Mahanthappa et al.[73] T_{ODT}'s for OSISO(0.35) and ISO12 ($f_O = 0.34$) were not accessed because thermal degradation occurs at the elevated temperatures required to disorder both polymers. The rationale for the higher T_{ODT}'s of the ABCBA pentablocks is presumably the same as that presented by Matsen and Thompson for AB diblocks and ABA triblocks;[21] the ABCBA pentablocks remain ordered to higher temperatures than the homologous ABC triblocks because a longer C chain must be dragged into the A and B domains to disorder the polymer in the pentablock case.

Only slight variations (±10%) in domain periodicity have been reported[15,22] for ABA triblocks and the homologous AB diblocks, a result in agreement with self-consistent-field theory calculations.[21] The comparison in domain spacing can be extended into ABCBA pentablocks and ABC triblocks. Both Mahanthappa et al.'s reported CPEPC/CPE domain periodicities,[73] and our OSISO/ISO values are relatively constant (±12%), a result generally expected on the basis of the AB/ABA precedent.

PEO Crystallinity. Bailey et al. measured the fractional crystallinity (X_c) of a series of ISO triblocks along the $f_I = f_S$ isopleth (including the lower molecular weight ISO triblocks listed in Table 1); X_c increased from 0 to ~0.55 as f_O changed from 0.05 to 0.12 and then remained constant at ~0.55 as f_O increased to 0.35.[24] The fractional crystallinity of 0.57 measured for the O^{70}-forming ISO-7a specimen is consistent with Bailey et al.'s results. The crystallinity of O^{70}-forming OSISO(0.13) is ~40% below the value measured by Bailey et al. for an ISO with a comparable f_O. This composition, however, is very close to the ISO phase boundary between LAM_2 and O^{70} and the associated rapid increase in X_c that occurs as PEO forms a relatively pure domain in the O^{70} mesostructure. We attribute the decrease in X_c for OSISO(0.13) to some mixing of the PS and PEO domains. X_c for LAM_3-forming OSISO(0.35) exceeds Bailey et al.'s previously reported values for ISO triblocks and is near the value for bulk PEO.[77]

Mechanical Properties. We can probe the consequences of attaching varying amounts of PEO to intrinsically tough SIS triblock by examining the tensile data of the OSISO series. The first comparison can be made between SIS and OSISO(0.06). Representative data are provided in Figure 5. Both polymers contain lamellae, but SIS has a 24% higher σ_{yield} and 72% larger ε_{fail} than OSISO(0.06). We suggest the differences in both values can be attributed to plasticization of the PS domain via mixing with the terminal PEO blocks. Several pieces of experimental data suggest the PS and PEO domains are mixed. First, the fractional PEO crystallinity of 0.06 in OSISO(0.06) is minimal, suggesting the PEO does not form pure domains. Second, the 002 reflection in the OSISO(0.06) SAXS data is extinct (see Figure 2), a result consistent with a LAM_2 microstructure comprised of alternating layers of PI and a PS/PEO mixture.[27] Furthermore, $\chi N_{SO} = 8.6$ for OSISO(0.06), and a neat SO diblock of this composition ($f_O = 0.11$) would not be expected to microphase-separate for χN_{SO} below ~50.[5] Both polymers yield and plastically deform, and SIS strain hardens, prior to failure.

Another relevant comparison can be made between OSISO(0.13) and OSISO(0.35). Sample OSISO(0.13) contains O^{70} while specimen OSISO(0.35) forms LAM_3; representative stress−strain curves for these two materials are provided in Figure 5. OSISO(0.13) yields and plastically deforms prior to failure, and the reduction in σ in the stress−strain curve at $\varepsilon \approx 0.06$ is indicative of necking. Necking has been reported in thermoplastic elastomers when a glassy domain is continuous in the loading direction. Dair et al., for instance, observed necking in SIS triblocks containing the Q^{230} morphology.[59,60] Necking in OSISO(0.13) is consistent with a continuous glassy PS domain created by the O^{70} morphology. In contrast to OSISO(0.13), OSISO(0.35) exhibits brittle failure at very low strains. We suggest that this drastically different behavior is the result of the different morphologies of the two samples; schematics of the LAM_3 and O^{70} mesostructures are depicted in Figure 6. In the LAM_3 morphology of sample OSISO(0.35), cracks can readily propagate across the two-dimensionally continuous PEO domains without encountering the SIS core material. As the cracks in the PEO fracture plane spread throughout the sample, there are no continuous glassy and rubbery domains to provide mechanical support and the sample fails. The OSISO(0.13) network, in contrast, has percolating PI, PS, and PEO domains; the [311] projection of the O^{70} unit cell is provided in Figure 6. Clearly, there is no fragile PEO bilayer in the O^{70} morphology of sample OSISO(0.13). As a result, a crack initiated in the PEO domain would have to split the tough SIS subdomains at every unit cell in order to traverse the material. Eliminating the fragile PEO bilayers by wrapping them into a three-dimensional network prevents failure at very low strains.

Here we note that samples OSISO(0.13) and OSISO(0.35) have different compositions and levels of PEO crystallinity (see Table 2). We suspect, on the basis of a previous report, that the increased PEO crystallinity of OSISO(0.35) compared to OSISO(0.13) does not cause the sharp decrease in toughness. Phatak and co-workers published a related study on the fracture properties of poly(ethylene-*b*-cyclohexylethylene-*b*-ethylene-*b*-cyclohexylethylene) (ECEC) tetrablock and ECECE pentablock copolymers.[78] All of the block copolymers examined by Phatak et al. contained an isotropic LAM_2 morphology. These materials, like the OSISO pentablocks, are comprised of an intrinsically tough ABA triblock with terminal semicrystalline blocks attached. The level of polyethylene (PE) crystallinity in the ECEC and ECECE samples ranged from 0.21 to 0.27, values below the PEO fractional crystallinity of 0.29 measured in sample OSISO(0.13). Even with these lower crystallinities, the

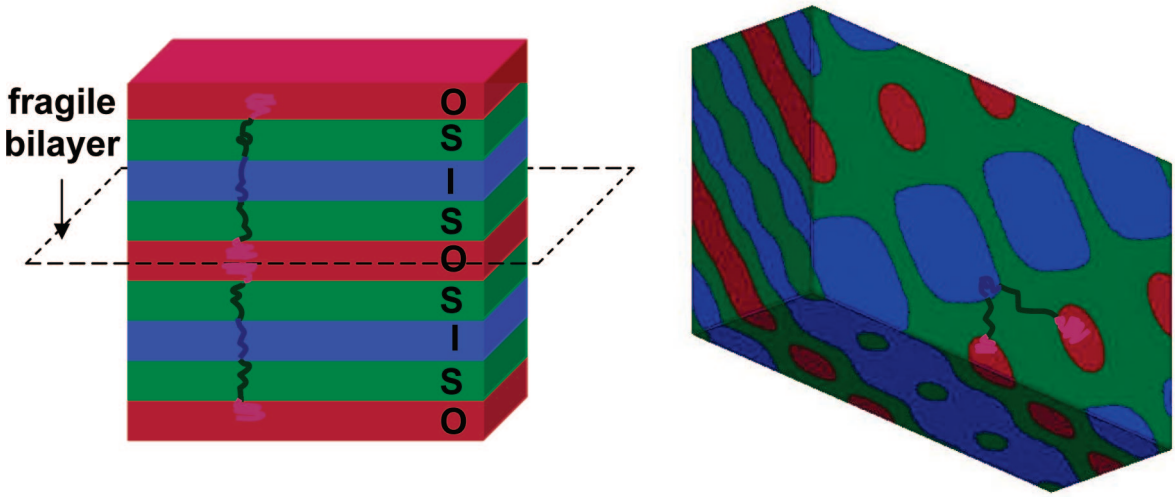

Figure 6. Schematics of the LAM_3 (left) and O^{70} (right) morphologies of samples OSISO(0.35) and OSISO(0.13). The LAM_3 mesostructure is a cartoon representation while the 311 projection of the O^{70} unit cell was generated using level-set modeling with $f_I \approx f_S$ and $f_O = 0.13$.[27] A crack can readily propagate through the fragile PEO bilayer in the LAM_3 microstructure. The 311 projection clearly shows that there are no fragile PEO bilayers in the O^{70} unit cell. As a result, the tough SIS subdomain that surrounds the PEO would have to be broken in order for a crack to traverse the O^{70} morphology.

isotropic lamellar ECEC and ECECE materials exhibited brittle behavior, effectively establishing a "threshold" of crystallinity at or above which brittle failure can result. The X_c of 0.29 in OSISO(0.13) is above this threshold, yet OSISO(0.13) does not fail in a brittle manner; we attribute the material's toughness to its network mesostructure. A more definitive conclusion would require a study of samples of the same polymer containing different morphologies. It might be possible to capture different morphologies by solvent-casting OSISO pentablocks from solvents of varying quality. This strategy has been successfully used in block copolymers[61,79] but has not yet been pursued for the ISO block terpolymers.

Comparison of the tensile data in Figure 5 for ISO-7a ($f_O = 0.15$) and OSISO(0.13) shows that the network morphology does not, by itself, prevent brittle failure. These samples have comparable compositions, overall molecular weights, and PEO crystallinities but differ in chain architecture. Clearly, chain architecture has a significant impact on the mechanical behavior of the materials. Cracks initiated in the PEO domain of ISO-7a can easily propagate because they can readily break the brittle IS subdomain. Sample OSISO(0.13), in contrast, contains a tough SIS thermoplastic elastomer that limits crack propagation and increases the toughness dramatically compared to the ISO triblock, with sharp increases in both the stress (σ_{fail}) and strain (ε_{fail}) at break. OSISO(0.13) yielded and plastically deformed prior to failure while ISO-7a fractured in a brittle fashion at very low strains. An intrinsically tough material with a brittle bilayer can be toughened by wrapping it into a network mesostructure; intrinsically brittle materials with a network microstructure are still brittle.

Conclusion

A synthetic strategy to prepare OSISO pentablock terpolymers with narrow molecular weight distributions in all blocks was presented. The morphologies of a symmetric SIS triblock and three OSISO pentablocks were characterized using SAXS, TEM, DMS, and DSC. The OSISO pentablocks are higher-order extensions of previously well-characterized ISO triblocks,[24,26,27] enabling us to experimentally compare the phase behavior of ABCBA pentablocks and the homologous ABC triblocks. The O^{70} network was identified in the OSISO pentablocks between LAM_2 and LAM_3, a morphology sequence identical to that observed in ISO triblocks. The identification of O^{70} in OSISO(0.13) demonstrates that the network mesostructures observed in ABC triblocks can be obtained in the higher-order symmetric ABCBA pentablocks.

Tensile testing was used to probe the mechanical consequences of adding various lengths of PEO chains to the ends of an intrinsically tough SIS thermoplastic elastomer. Sample OSISO(0.35) contained the LAM_3 microstructure and had semicrystalline terminal PEO blocks; the PEO bilayer led to fracture in a brittle fashion at very low strains, a result consistent with the work of Phatak and co-workers.[78] OSISO(0.13), in contrast, contained the O^{70} network and had a strain at failure of 1.3, even though the crystallinity of the terminal PEO blocks was above the brittle threshold established by Phatak et al. This improved toughness is attributed to the triply continuous nature of the O^{70} morphology and demonstrates that an intrinsically robust material with a fragile bilayer can be toughened by wrapping it into a three-dimensional network. The OSISO network is much tougher than the ISO counterpart, suggesting that pentablock terpolymers could prove useful in applications requiring tough, multiply continuous morphologies (e.g., use as a separation membrane).

Acknowledgment. The authors gratefully acknowledge financial support from the NSF through Grant DMR-0220460 from the Department of Energy through Grant 5-35908. We also acknowledge partial support from the National Science Foundation Materials Research Science and Engineering Center (NSF-MRSEC) at the University of Minnesota (NSF DMR-0212302). Graduate fellowships to A.J.M. from the Department of Homeland Security and the Department of Defense are gratefully acknowledged. Portions of this work were performed at the DuPont−Northwestern−Dow Collaborative Access Team (DND-CAT) located at Sector 5 of the Advanced Photon Source (APS). DND-CAT is supported by E.I. DuPont de Nemours & Co., The Dow Chemical Company, and the State of Illinois. Use of the Advanced Photon Source (APS) was supported by the U.S. Department of Energy, Office of Science, Office of Basic Energy Sciences, under Contract DE-AC02-06CH11357. Parts of this work were carried out in the University of Minnesota Institute of Technology Characterization Facility, which receives partial support from NSF through the NNIN program. We thank Professor Eric W. Cochran for letting us use his level-set software and thank Michael J. Bluemle for his help in running the software and generating the level-set projection provided in Figure 6.

References and Notes

(1) Leibler, L. *Macromolecules* **1980**, *13*, 1602–1617.
(2) Bates, F. S.; Fredrickson, G. H. *Annu. Rev. Phys. Chem.* **1990**, *41*, 525–557.
(3) Khandpur, A. K.; Förster, S.; Bates, F. S.; Hamley, I. W.; Ryan, A. J.; Bras, W.; Almdal, K.; Mortensen, K. *Macromolecules* **1995**, *28*, 8796–8806.
(4) Matsen, M. W.; Bates, F. S. *Macromolecules* **1996**, *29*, 1091–1098.
(5) Cochran, E. W.; Garcia-Cervera, C. J.; Fredrickson, G. H. *Macromolecules* **2006**, *39*, 2449–2451.
(6) Hahn, T., Ed. *International Tables for Crystallography*, 4th revised ed.; **1994**; Vol. *A*.
(7) Tyler, C. A.; Morse, D. C. *Phys. Rev. Lett.* **2005**, *94*, 208302.
(8) Takenaka, M.; Wakada, T.; Akasaka, S.; Nishitsuji, S.; Saijo, K.; Shimizu, H.; Kim, M. I.; Hasegawa, H. *Macromolecules* **2007**, *40*, 4399–4402.
(9) Tyler, C. A.; Qin, J.; Bates, F. S.; Morse, D. C. *Macromolecules* **2007**, *40*, 4654–4668.
(10) Helfand, E.; Wasserman, Z. R. *Macromolecules* **1976**, *9*, 879–888.
(11) Mayes, A. M.; Olvera de la Cruz, M. *J. Chem. Phys.* **1989**, *91*, 7228–7235.
(12) Mayes, A. M.; Olvera de la Cruz, M. *J. Chem. Phys.* **1991**, *95*, 4670–4677.
(13) Gehlsen, M. D.; Almdal, K.; Bates, F. S. *Macromolecules* **1992**, *25*, 939–943.
(14) Adams, J. L.; Graessley, W. W.; Register, R. A. *Macromolecules* **1994**, *27*, 6026–6032.
(15) Matsushita, Y.; Nomura, M.; Watanabe, J.; Mogi, Y.; Noda, I.; Imai, M. *Macromolecules* **1995**, *28*, 6007–6013.
(16) McKay, K. W.; Gros, W. A.; Diehl, C. F. *J. Appl. Polym. Sci.* **1995**, *56*, 947–958.
(17) Ryu, C. Y.; Lee, M. S.; Hajduk, D. A.; Lodge, T. P. *J. Polym. Sci., Part B* **1997**, *35*, 2811–2823.
(18) Avgeropoulos, A.; Dair, B. J.; Hadjichristidis, N.; Thomas, E. L. *Macromolecules* **1997**, *30*, 5634–5642.
(19) Laurer, J. H.; Hajduk, D. A.; Fung, J. C.; Sedat, J. W.; Smith, S. D.; Gruner, S. M.; Agard, D. A.; Spontak, R. J. *Macromolecules* **1997**, *30*, 3938–3941.
(20) Mani, S.; Weiss, R. A.; Cantino, M. E.; Khairallah, L. H.; Hahn, S. F.; Williams, C. E. *Eur. Polym. J.* **1999**, *36*, 215–219.
(21) Matsen, M. W.; Thompson, R. B. *J. Chem. Phys.* **1999**, *111*, 7139–7146.
(22) Mai, S.; Mingvanish, W.; Turner, S. C.; Chaibundit, C.; Fairclough, J. P. A.; Heatley, F.; Matsen, M. W.; Ryan, A. J.; Booth, C. *Macromolecules* **2000**, *33*, 5124–5130.
(23) Bates, F. S.; Fredrickson, G. H. *Phys. Today* **1999**, *52*, 32–38.
(24) Bailey, T. S.; Hardy, C. M.; Epps, T. H., III; Bates, F. S. *Macromolecules* **2002**, *35*, 7007–7017.
(25) Epps, T. H., III; Bailey, T. S.; Waletzko, R.; Bates, F. S. *Macromolecules* **2003**, *36*, 2873–2881.
(26) Epps, T. H., III; Cochran, E. W.; Hardy, C. M.; Bailey, T. S.; Waletzko, R. S.; Bates, F. S. *Macromolecules* **2004**, *37*, 7085–7088.
(27) Epps, T. H., III; Cochran, E. W.; Bailey, T. S.; Waletzko, R. S.; Hardy, C. M.; Bates, F. S. *Macromolecules* **2004**, *37*, 8325–8341.
(28) Epps, T. H., III; Chatterjee, J.; Bates, F. S. *Macromolecules* **2005**, *38*, 8775–8784.
(29) Epps, T. H., III; Bates, F. S. *Macromolecules* **2006**, *39*, 2676–2682.
(30) Chatterjee, J.; Jain, S.; Bates, F. S. *Macromolecules* **2007**, *40*, 2882–2896.
(31) Meuler, A. J.; Ellison, C. J.; Evans, C. M.; Hillmyer, M. A.; Bates, F. S. *Macromolecules* **2007**, *40*, 7072–7074.
(32) Frielinghaus, H.; Hermsdorf, N.; Almdal, K.; Mortensen, K.; Messe, L.; Corvazier, L.; Fairclough, J. P. A.; Ryan, A. J.; Olmsted, P. D.; Hamley, I. W. *Europhys. Lett.* **2001**, *53*, 680–686.
(33) Bailey, T. S.; Pham, H. D.; Bates, F. S. *Macromolecules* **2001**, *34*, 6994–7008.
(34) Qin, J.; Bates, F. S.; Morse, D. C. Manuscript in preparation.
(35) Shefelbine, T. A.; Vigild, M. E.; Matsen, M. W.; Hajduk, D. A.; Hillmyer, M. A.; Cussler, E. L.; Bates, F. S. *J. Am. Chem. Soc.* **1999**, *121*, 8457–8465.
(36) Goldacker, T.; Abetz, V. *Macromolecules* **1999**, *32*, 5165–5167.
(37) Suzuki, J.; Seki, M.; Matsushita, Y. *J. Chem. Phys.* **2000**, *112*, 4862–4868.
(38) Hueckstaedt, H.; Goldacker, T.; Goepfert, A.; Abetz, V. *Macromolecules* **2000**, *33*, 3757–3761.
(39) Hardy, C. M.; Bates, F. S.; Kim, M.; Wignall, G. D. *Macromolecules* **2002**, *35*, 3189–3197.
(40) Cochran, E. W.; Bates, F. S. *Phys. Rev. Lett.* **2004**, *93*, 087802.
(41) Urbas, A. M.; Maldovan, M.; DeRege, P.; Thomas, E. L. *Adv. Mater.* **2002**, *14*, 1850–1853.
(42) Hillmyer, M. A. *Adv. Polym. Sci.* **2005**, *190*, 137–181.
(43) Yang, S. Y.; Ryu, I.; Kim, H. Y.; Kim, J. K.; Jang, S. K.; Russell, T. P. *Adv. Mater.* **2006**, *18*, 709–712.
(44) Phillip, W. A.; Rzayev, J.; Hillmyer, M. A.; Cussler, E. L. *J. Membr. Sci.* **2006**, *286*, 144–152.
(45) Kopchick, J. G.; Storey, R. F.; Beyer, F. L.; Mauritz, K. A. *Polymer* **2007**, *48*, 3739–3748.
(46) Mao, H.; Hillmyer, M. A. *Macromolecules* **2005**, *38*, 4038–4039.
(47) Mao, H.; Hillmyer, M. A. *Soft Matter* **2006**, *2*, 57–59.
(48) Ruzette, A. G.; Soo, P. P.; Sadoway, D. R.; Mayes, A. M. *J. Electrochem. Soc.* **2001**, *148*, A537–A543.
(49) Vorrey, S.; Teeters, D. *Electrochim. Acta* **2003**, *48*, 2137–2141.
(50) Singh, M.; Odusanya, O.; Wilmes, G. M.; Eitouni, H. B.; Gomez, E. D.; Patel, A. J.; Chen, V. L.; Park, M. J.; Fragouli, P.; Iatrou, H.; Hadjichristidis, N.; Cookson, D.; Balsara, N. P. *Macromolecules* **2007**, *40*, 4578–4585.
(51) Ndoni, S.; Papadakis, C. M.; Bates, F. S.; Almdal, K. *Rev. Sci. Instrum.* **1995**, *66*, 1090–1095.
(52) Meuler, A. J.; Mahanthappa, M. K.; Hillmyer, M. A.; Bates, F. S. *Macromolecules* **2007**, *40*, 760–762.
(53) Lo, G. Y.; Otterbacher, E. W.; Gatzke, A. L.; Tung, L. H. *Macromolecules* **1994**, *27*, 2233–2240.
(54) Hillmyer, M. A.; Bates, F. S. *Macromolecules* **1996**, *29*, 6994–7002.
(55) Fetters, L. J.; Lohse, D. J.; Richter, D.; Witten, T. A.; Zirkel, A. *Macromolecules* **1994**, *27*, 4639–4647.
(56) Rosedale, J. H.; Bates, F. S. *Macromolecules* **1990**, *23*, 2329–2338.
(57) Kossuth, M. B.; Morse, D. C.; Bates, F. S. *J. Rheol.* **1999**, *43*, 167–196.
(58) Wunderlich, B. *Macromolecular Physics*; Academic Press: New York, 1980; Vol. *3*.
(59) Dair, B. J.; Honeker, C. C.; Alward, D. B.; Avgeropoulos, A.; Hadjichristidis, N.; Fetters, L. J.; Capel, M.; Thomas, E. L. *Macromolecules* **1999**, *32*, 8145–8152.
(60) Dair, B. J.; Avgeropoulos, A.; Hadjichristidis, N.; Thomas, E. L. *J. Mater. Sci.* **2000**, *35*, 5207–5213.
(61) Qiao, L.; Leibig, C.; Hahn, S. F.; Winey, K. I. *Ind. Eng. Chem. Res.* **2006**, *45*, 5598–5602.
(62) Sha, K.; Li, D.; Li, Y.; Zhang, B.; Wang, J. *Macromolecules* **2008**, *41*, 361–371.
(63) Bailey, T. S.; Rzayev, J.; Hillmyer, M. A. *Macromolecules* **2006**, *39*, 8772–8781.
(64) Vazaios, A.; Pitsikalis, M.; Hadjichristidis, N. *J. Polym. Sci., Part A: Polym. Chem.* **2003**, *41*, 3094–3102.
(65) Toman, L.; Janata, M.; Spevacek, J.; Vlcek, P.; Latalova, P.; Masar, B.; Sikora, A. *J. Polym. Sci., Part A: Polym. Chem.* **2004**, *42*, 6098–6108.
(66) Toman, L.; Janata, M.; Spevacek, J.; Vlcek, P.; Latalova, P.; Sikora, A.; Masar, B. *J. Polym. Sci., Part A: Polym. Chem.* **2005**, *43*, 3823–3830.
(67) Ling, J.; Chen, W.; Shen, Z. *J. Polym. Sci., Part A: Polym. Chem.* **2005**, *43*, 1787–1796.
(68) Determan, M. D.; Cox, J. P.; Seifert, S.; Thiyagarajan, P.; Mallapragada, S. K. *Polymer* **2005**, *46*, 6933–6946.
(69) Storey, R. F.; Scheuer, A. D.; Achord, B. C. *J. Macromol. Sci., Part A: Pure Appl. Chem.* **2006**, *43*, 1493–1512.
(70) Thunemann, A. F.; Kubowicz, S.; von, B. H.; Mohwald, H. *Langmuir* **2006**, *22*, 2506–2510.
(71) Peleshanko, S.; Anderson, K. D.; Goodman, M.; Determan, M. D.; Mallapragada, S. K.; Tsukruk, V. V. *Langmuir* **2007**, *23*, 25–30.
(72) Triftaridou, A. I.; Vamvakaki, M.; Patrickios, C. S. *Biomacromolecules* **2007**, *8*, 1615–1623.
(73) Mahanthappa, M. K.; Lim, L. S.; Hillmyer, M. A.; Bates, F. S. *Macromolecules* **2007**, *40*, 1585–1593.
(74) Mahanthappa, M. K.; Hillmyer, M. A.; Bates, F. S. *Macromolecules* **2008**, *41*, 1341–1351.
(75) He, Y.; Lodge, T. P. *Macromolecules* **2008**, *41*, 167–174.
(76) Stavrouli, N.; Katsampas, I.; Aggelopoulos, S.; Tsitsilianis, C. *Macromol. Rapid Commun.* **2008**, *29*, 130–135.
(77) Li, X.; Hsu, S. L. *J. Polym. Sci., Polym. Phys.* **1984**, *22*, 1331–1342.
(78) Phatak, A.; Lim, L. S.; Reaves, C. K.; Bates, F. S. *Macromolecules* **2006**, *39*, 6221–6228.
(79) Sakurai, S.; Sakamoto, J.; Shibayama, M.; Nomura, S. *Macromolecules* **1993**, *26*, 3351–3356.

MA800885S